A Mechanistic Study of Isopenicillin N Formation Using Density Functional Theory

Maria Wirstam* and Per E. M. Siegbahn

Contribution from the Department of Physics, Stockholm University, Box 6730, S-113 85 Stockholm, Sweden

Received March 29, 2000. Revised Manuscript Received June 26, 2000

Abstract: The catalytic mechanism of isopenicillin N formation by isopenicillin N synthase has been investigated using the density functional theory method B3LYP. The catalytic cycle is suggested to occur in 12 steps, where the closure of the four-membered β-lactam ring precedes the closure of the five-membered thiazolidine ring. Two of the reaction steps were found to have significant barriers of similar size, in line with experimental suggestions that these steps are rate-determining. One of these steps is the hydrogen atom transfer from the cysteinyl β-carbon, leading to formation of an oxo-ferryl complex and, in a subsequent step, to formation of the monocyclic β-lactam ring. The other significant barrier is obtained for the hydrogen atom transfer from the β-carbon of the valinyl group to the oxo-ligand of IPNS, initiating the formation of the thiazolidine ring. The last step of the catalytic reaction, which completes the closure of the thiazolidine ring by a bond formation between the Val-β-carbon and the Cys-sulfur, was found to be very exothermic. An important aspect obtained from the calculations is that the dioxygen ligand needs to be protonated prior to the Cys-β-C-H activation. Otherwise, this step would not be partly rate-limiting and would thus be in conflict with isotope experiments.

I. Introduction

Isopenicillin N synthase (IPNS) is a mononuclear non-heme iron enzyme that plays an important role in the biosynthesis of antibiotics.[1] By use of one O_2 molecule, the enzyme catalyzes the bicyclic ring closure of the substrate δ-(L-α-aminoadipoyl)-L-cysteinyl-*d*-valine (ACV) to form two water molecules and isopenicillin N (IPN), a precursor of the antibiotics penicillins and cephalosporins.[1−3] Due to their outstanding importance in medicine, it is of interest to understand the mechanisms for formation of these antibiotics. Before the first X-ray crystal structure of IPNS was obtained spectroscopic data from Mössbauer,[4,5] EPR,[4−6] NMR,[6,7] EXAFS,[8,9] and optical spectroscopy[4,5,6] were used to investigate the active site, suggesting the presence of a ferrous iron center coordinating to one aspartate, three histidine residues, and two OH/H_2O ligands in the resting state.[10] Later, site-directed mutagenesis experiments showed that among seven conserved histidine residues, only two are essential for catalytic activity.[11−13] These two histidine residues are observed in ESEEM studies of Cu(II)-IPNS.[14] Furthermore, there are two conserved cysteine residues but mutagenesis showed that neither of them is essential for catalysis.[15,16] Recently, the X-ray crystal structure was obtained for IPNS of Aspergillus nidulans, complexed with manganese instead of iron. The crystal structure shows that the metal is octahedrally coordinated by two histidines (His 214 and His 270), one aspartate (Asp 216), one glutamine (Gln 330), and two water molecules[11] (see Figure 1a). In the presence of the substrate ACV, Gln 330 loses its coordination to iron and is replaced by

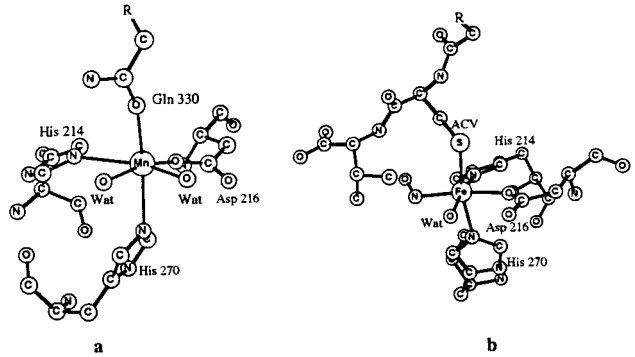

Figure 1. (a) Resting ferrous state of IPNS with Fe substituted by Mn (1IPS).[11] (b) IPNS complexed with ACV and NO (1BLZ).[17]

(1) Baldwin, J. E.; Abraham, E. *Nat. Prod. Rep.* **1988**, *5*, 129−145.
(2) White, R. L.; John, E. M.; Baldwin, J. E.; Abraham, E. P. *Biochem. J.* **1982**, *203*, 791−793.
(3) Bainbridge, Z. A.; Scott, R. I.; Perry, D. *J. Chem. Technol. Biotechnol.* **1992**, *55*, 233−238.
(4) Chen, V. J.; Orville, A. M.; Harpel, M. R.; Frolik, C. A.; Surerus, K. K.; Munck, E.; Lipscomb, J. D. *J. Biol. Chem.* **1989**, *264*, 21677−21681.
(5) Orville, A. M.; Chen, V. J.; Kriauciunas, A.; Harpel, M. R.; Fox, B. G.; Munck, E.; Lipscomb, J. D. *Biochemistry* **1992**, *31*, 4602−4612.
(6) Ming, L. J.; Que, L.; Kriauciunas, A.; Frolik, C. A.; Chen, V. J. *Inorg. Chem.* **1990**, *29*, 1111−1112.
(7) Ming, L. J.; Que, L.; Kriauciunas, A.; Frolik, C. A.; Chen, V. J. *Biochemistry* **1991**, *30*, 11653−11659.
(8) Scott, R. A.; Wang, S. K.; Eidsness, M. K.; Kriauciunas, A.; Frolik, C. A.; Chen, V. J. *Biochemistry* **1992**, *31*, 4596−4601.
(9) Randall, C. R.; Zang, Y.; True, A. E.; Que, L.; Charnock, J. M.; Garner, C. D.; Fujishima, Y.; Schofield, C. J.; Baldwin, J. E. *Biochemistry* **1993**, *32*, 6664−6673.
(10) Feig, A. L.; Lippard, S. J. *Chem. Rev.* **1994**, *94*, 759−805.
(11) Roach, P. L.; Clifton, I. J.; Fülöp, V.; Harlos, K.; Barton, G. J.; Hajdu, J.; Andersson, I.; Schofield, C. J.; Baldwin, J. E. *Nature* **1995**, *375*, 700−704.
(12) Borovok, I.; Landman, O.; Kreisberg-Zakarin, R.; Aharonowitz, Y.; Cohen, G. *Biochemistry* **1996**, *35*, 1981−1987.
(13) Tan, D. S. H.; Sim, T.-S. *J. Biol. Chem.* **1996**, *271*, 889−894.
(14) Jiang, F.; Peisach, J.; Ming, L. J.; Que, L.; Chen, V. J. *Biochemistry* **1991**, *30*, 11437−11445.
(15) Samson, S. M.; Chapman, J. L.; Belagaje, R.; Queener, S. W.; Ingolia, T. D. *Proc. Natl. Acad. Sci. U.S.A.* **1987**, *84*, 5705−5709.
(16) Kriauciunas, A.; Frolik, C. A.; Hassell, T. C.; Skatrud, P. L.; Johnson, M. G.; Holbrook, N. L.; Chen, V. J. *J. Biol. Chem.* **1991**, *266*, 11779−11788.

10.1021/ja001103k CCC: $19.00 © 2000 American Chemical Society
Published on Web 08/19/2000

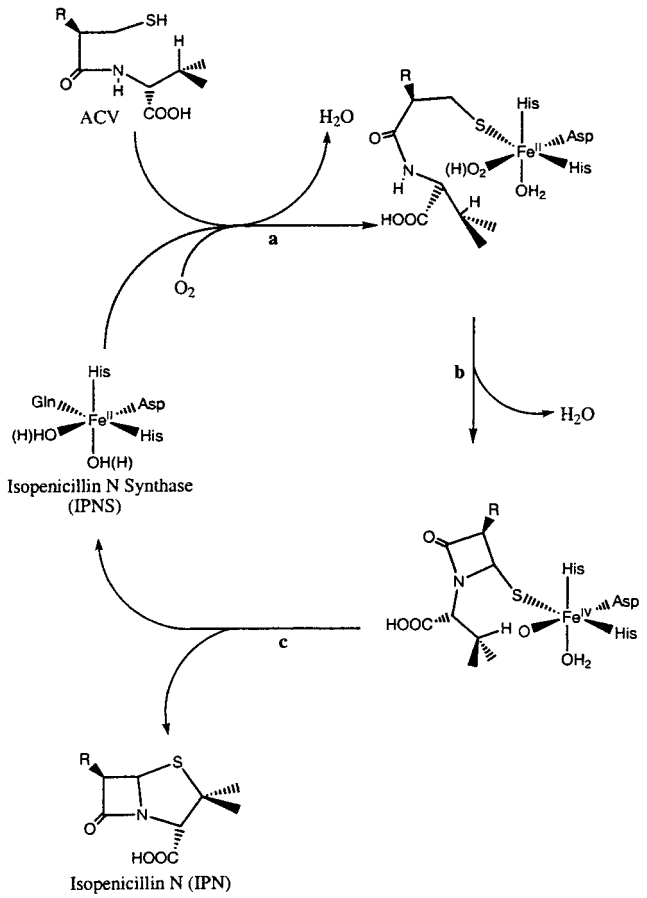

Figure 2. Catalytic cycle of IPN formation by IPNS.

the thiolate of ACV as shown from the X-ray crystal structure obtained for Fe(II)-containing IPNS complexed with ACV.[17] Direct interaction between the substrate and iron is also implied from spectroscopic changes at the iron center.[4−9] When exposed to the molecular oxygen analogue NO, EPR studies[5] indicate that NO binds to the Fe(II) complex, giving an octahedral coordination. The crystal structure of this complex[17] shows that NO binds trans to Asp 216 in a nonlinear orientation, which should be a likely binding site also for O_2 (see Figure 1b).

On the basis of substrate analogues and isotopic labeling experiments, a catalytic mechanism for IPNS as shown in Figure 2 was first proposed by Baldwin et al.[18,19] Additional experimental data, giving a more detailed picture of the enzyme mechanism, have then been gathered in three recent reviews.[10,20,21] The binding of the substrate and molecular oxygen into the enzyme leads to loss of one water molecule (Figure 2a). In the subsequent step, the Cys-β-C-H hydrogen of ACV migrates to the dioxygen, leading to formation of the oxo-ferryl:β-lactam ring intermediate and a second water molecule (Figure 2b).

Spectroscopic[18,19] and crystallographic[22] studies have indicated that the closure of the β-lactam ring occurs prior to that of the thiazolidine ring, which completes the formation of the bicyclic structure of isopenicillin N. The X-ray crystallographic studies show that when the natural substrate ACV was used, the β-lactam ring could not be observed and instead the reaction led directly to formation of bicyclic IPN. If, on the other hand, the substrate analogue δ-(L-α-aminoadipoyl)-L-cysteinyl-L-*S*-methyl-cysteine (ACMC) was used, the reaction could be interrupted after the formation of the monocyclic β-lactam intermediate.

In the final step of the reaction (Figure 2c), the oxo ligand on iron abstracts a hydrogen atom from the Val-β-carbon, which instead binds to the Cys sulfur, forming IPN complexed with IPNS as shown from the X-ray crystal structure.[22]

Although there is a general agreement on the fundamental steps of the catalytic cycle shown in Figure 2, many mechanistic details are still not fully understood. The DFT-B3LYP method has successfully been used to investigate the reaction mechanisms of other metalloenzymes and in particular other O−O splitting Fe-containing enzymes.[23−26] In the present study, the reaction cycle presented in Figure 2 is investigated step by step by determining all possible transition states and intermediates. In the proposed mechanism, similar to that previously suggested,[18,19] the reaction passes through eleven intermediates and transition states from the O_2:IPNS:Fe:ACV to the H_2O:IPNS:Fe:IPN complex (Figure 2b,c). All intermediates and transition states were geometry optimized and a potential energy surface for the reaction was obtained. On the basis of the calculated results, many features, such as relative energies, geometries, and charge and spin populations of each reaction step of the catalytic cycle shown in Figure 2, could be analyzed in detail. Furthermore, some new proposals concerning the mechanism could be made based on the energetic data obtained.

II. Computational Details

The calculations were performed in two steps. First, an optimization of the geometry was performed using the B3LYP method.[27,28] Double-ζ basis sets were used in this step. In the second step the energy was evaluated for the optimized geometry using large basis sets including diffuse functions and with a single set of polarization functions on each atom. The final energy evaluation was also performed at the B3LYP level. All the calculations were carried out using the GAUSSIAN programs.[29,30]

In the B3LYP geometry optimizations, the LANL2DZ set of the GAUSSIAN program was used. For iron this means that a nonrelativistic effective core potential (ECP) according to Hay and Wadt[31] was used. The valence basis set used in connection with this ECP is essentially of double-ζ quality. The rest of the atoms are described by standard double-ζ basis sets. To obtain the transition states, the main parameters were first frozen at different values, optimizing all other

(17) Roach, P. L.; Clifton, I. J.; Hensgens, C. M. H.; Shibata, N.; Schofield, C. J.; Hajdu, J.; Baldwin, J. E. *Nature* **1997**, *387*, 827−830.
(18) Baldwin, J. E.; Bradley, M. *Chem. Rev.* **1990**, *90*, 1079−1088.
(19) Baldwin, J. E.; Lynch, G. P.; Schofield, C. J. *Tetrahedron* **1992**, *48*, 9085−9100.
(20) Que, L. Jr.; Ho, R. Y. N. *Chem. Rev.* **1996**, *96*, 2607−2624.
(21) Solomon, E. I.; Brunold, T. C.; Davis, M. I.; Kemsley, J. N.; Lee, S.-K.; Lehnert, N.; Neese, F.; Skulan, A. J.; Yang, Y.-S.; Zhou, J. *Chem. Rev.* **2000**, *100*, 235−349.
(22) Burzlaff, N. I.; Rutledge, P. J.; Clifton, I. J.; Hensgens, C. M. H.; Pickford, M.; Adlington, R. M.; Roach, P. L.; Baldwin, J. E. *Nature* **1999**, *401*, 721−724.
(23) Wirstam, M.; Blomberg, M. R. A.; Siegbahn, P. E. M. *J. Am. Chem. Soc.* **1999**, *121*, 10178−10185.
(24) Blomberg, M. R. A.; Siegbahn, P. E. M.; Babcock, G. T.; Wikström, M. *J. Inorg. Biochem.* In press.
(25) Siegbahn, P. E. M. *J. Inorg. Chem.* **1999**, *38*, 2880−2889.
(26) Siegbahn, P. E. M.; Blomberg, M. R. A. In *Theoretical Chemistry − Processes and Properties of Biological Systems*; Eriksson, L. A., Ed.; Elsevier: Amsterdam, submitted.
(27) Becke, A. D. *Phys. Rev.* **1988**, *A38*, 3098. Becke, A. D. *J. Chem. Phys.* **1993**, *98*, 1372. Becke, A. D. *J. Chem. Phys.* **1993**, *98*, 5648.
(28) Stevens, P. J.; Devlin, F. J.; Chablowski, C. F.; Frisch, M. J. *J. Phys. Chem.* **1994**, *98*, 11623.
(29) Frisch, M. J.; Trucks, G. W.; Schlegel, H. B.; Gill, P. M. W.; Johnson, B. G.; Robb, M. A.; Cheeseman, J. R.; Keith, T.; Petersson, G. A.; Montgomery, J. A.; Raghavachari, K.; Al-Laham, M. A.; Zakrzewski, V. G.; Ortiz, J. V.; Foresman, J. B.; Cioslowski, J.; Stefanov, B. B.; Nanayakkara, A.; Challacombe, M.; Peng, C. Y.; Ayala, P. Y.; Chen, W.; Wong, M. W.; Andres, J. L.; Replogle, E. S.; Gomperts, R.; Martin, R. L.; Fox, D. J.; Binkley, J. S.; Defrees, D. J.; Baker, J.; Stewart, J. P.; Head-Gordon, M.; Gonzalez, C.; Pople, J. A. *Gaussian 94*, Revision B.2; Gaussian Inc.: Pittsburgh, PA, 1995.

degrees of freedom. In the transition state region, a Hessian was calculated at the same level as used for the geometry optimization. Using this Hessian a full transition state geometry optimization was performed. If the geometry or the energy was significantly changed during the transition state optimization a second Hessian calculation was performed in the converged geometry to verify that one imaginary frequency was obtained corresponding to the right parameter for the reaction step. All transition states were found to have one imaginary frequency as they should except one where a distance was frozen during the transition state optimization as will be discussed below. In that case, one small additional imaginary frequency was obtained.

Where not otherwise stated, all geometries are fully optimized. For some structures freezing one parameter turned out to be necessary to avoid large structural changes of the ACV analogue, believed to be artifacts of the model. The available X-ray crystal strctures of the substrate bound enzyme[17,22] reveal that ACV is held in its position by hydrogen bonds between its polar groups and the surrounding amino acids and water molecules. Furthermore, the structures show that the orientation of ACV only differs slightly in the different intermediates located. If all parameters are fully optimized unrealistic structural distortions of the substrate occur for some of the intermediates since the hydrogen bonds present in the protein are not included in the quantum chemical model. These distortions are in conflict with the crystal structures and therefore a freezing procedure was used for these intermediates (see further the discussion below).

In the B3LYP energy calculations the diffuse and polarization functions from the 6-311+G(1d,1p) basis sets in the GAUSSIAN program were added to the LANL2DZ basis sets. This basis set has a single set of polarization functions on all atoms including f-sets on iron, and also diffuse functions.

Zero-point effects were computed and added to the final energies for some of the reaction steps, in most cases using smaller model-clusters than the ones that will be described below. The zero-point corrections were found to be rather small, in the range 0−2 kcal/mol. For one reaction barrier involving the activation of the Cys-β-C−H bond using a positively charged cluster, a larger zero-point effect of −5.1 kcal/mol was obtained. For this step, the frequency calculation was performed using the large model cluster.

Electrostatic interactions between the quantum chemical model and the surrounding residues were not included in the calculations for technical reasons. However, these effects have in previous studies on other enzymatic systems been shown to be rather insignificant as long as only energies of clusters that have the same charge are compared. Normally, the dielectric effects on the relative energies are in the range 0−5 kcal/mol for proteins.[32−36] As will be described below, the mechanisms that are ruled out in the present study were found to differ from experimental activation energies by 15 and 17 kcal/mol, respectively, while the proposed mechanism has activation energies very close to the experimental values (within 3 kcal/mol). The different mechanisms investigated are thus distinguished by energy values that are much larger than the expected solvent effects. Therefore, inclusion of these effects should not significantly change any conclusions made concerning the reaction mechanism of IPNS.

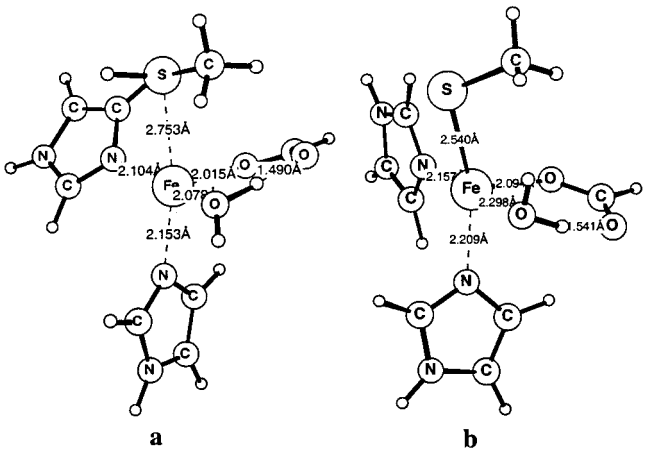

Figure 3. Structures for IPNS complexed with ACV Optimized [5]A for the cases when (a) the proton remains on the thiol group of ACV upon complexation, giving a net charge of the cluster of +1, and (b) when the thiol group is deprotonated, resulting in a neutral cluster.

III. Results and Discussion

The X-ray crystal structure for the manganese-substituted IPNS resting state (Figure 1a) shows that Mn(II) is ligated by two oxygen-containing groups. The metal−oxygen bond distances of 2.27 and 2.26 Å, respectively,[11] indicates two water ligands. To obtain a metal oxidation state of II, this compound is best described by a model cluster with a net charge of +1. In the first step of the catalytic cycle, Figure 2 step a, the thiol group of ACV replaces Gln 330 and one of the water molecules leaves the structure, followed by a change in the metal coordination geometry from octahedral to square pyramidal.[17] In the absence of O_2 or NO, the thiol group of ACV could donate its SH proton to a basic group upon coordination to iron. The X-ray crystal structure obtained for IPNS complexed with ACV[17] reveals the presence of a hydrogen bond chain of 3 water molecules, connecting the thiol group and the terminal carboxylate group of ACV. One possibility is a proton transfer from the thiolate to the carboxylate when ACV binds to iron. Alternatively, another group accepts the proton or the proton remains on the sulfur. A fully optimized [ACV-SH:Fe(II)IPNS]$^+$ model containing a protonated ACV-thiol, replaced by a $HSCH_3$ group, is shown in Figure 3a. The main difference between the theoretical and the experimental structure concerns the Fe−S distance, which was determined to be 2.75 Å in the optimized geometry and only 2.41 Å in the experimental structure. However, also if the thiol group is deprotonated, giving a neutral [ACV-S:Fe(II)IPNS]^0 model cluster, the optimized Fe−S distance of 2.54 Å is slightly longer than what was found in the crystal structure (see Figure 3b). The above results obtained for the ACV-IPNS model clusters thus indicate that a protonated thiol gives a Fe−S distance that is too long while a deprotonated thiol gives better agreement with the X-ray crystal structure.

In the next step of the catalytic cycle, O_2 binds to iron. The subsequent steps, b−c of the catalytic cycle of IPNS shown in Figure 1, have been the main interest in the present study. These reaction steps include the O−O cleavage of molecular oxygen and the stepwise formation of the bicyclic ring.

In the present study, two different mechanisms for formation of the monocyclic β-lactam ring from the O_2:IPNS:ACV complex were investigated, both of them resembling the ones previously proposed based on crystallographic and spectroscopic

(30) Frisch, M. J.; Trucks, G. W.; Schlegel, H. B.; Scuseria, G. E.; Robb, M. A.; Cheeseman, J. R.; Zakrzewski, V. G.; Montgomery, J. A., Jr.; Stratmann, R. E.; Burant, C. J.; Dapprich, S.; Millam, J. M.; Daniels, A. D.; Kudin, K. N.; Strain, M. C.; Farkas, O.; Tomasi, J.; Barone, V.; Cossi, M.; Cammi, R.; Mennucci, B.; Pomelli, C.; Adamo, C.; Clifford, S.; Ochterski, J.; Petersson, A. G.; Ayala, Y. P.; Cui, Q.; Morokuma, K.; Malick, K. D.; Rabuck, D. A.; Raghavachari, K.; Foresman, B. J.; Cioslowski, J.; Ortiz, V. J.; Stefanov, B. B.; Liu, G.; Liashenko, A.; Piskorz, P.; Komaromi, I.; Gomperts, R.; Martin, L. R.; Fox, J. D.; Keith, T.; Al-Laham, A. M.; Peng, Y. C.; Nanayakkara, A.; Gonzalez, C.; Challacombe, M.; Gill, P. M. W.; Johnson, B.; Chen, W.; Wong, M. W.; Andres, J. L.; Gonzalez, C.; Head-Gordon, M.; Replogle, E. S.; Pople, J. A. *Gaussian 98*, Revision A.3; Gaussian, Inc.; Pittsburgh, PA, 1998.

(31) Hay, P. J.; Wadt, W. R. *J. Chem. Phys.* **1985**, *82*, 299.

(32) Pavlov, M.; Blomberg, M. R. A.; Siegbahn, P. E. M. *Int. J. Quantum Chem.* **1998**, *73*, 197−207.

(33) Siegbahn, P. E. M. *J. Am. Chem. Soc.* **1998**, *120*, 8417−8429.

(34) Prabhakar, R.; Blomberg, M. R. A.; Siegbahn, P. E. M. *Theor. Chem. Acc.* In press.

(35) Siegbahn, P. E. M.; Blomberg, M. R. A. *Chem. Rev.* **2000**, *100*, 421−437.

(36) Siegbahn, P. E. M.; Blomberg, M. R. A. *Annu. Rev. Phys. Chem.* **1999**, *50*, 221−249.

data.[18,19] In one of the mechanisms studied, the ACV-thiol proton leaves the iron center of IPNS upon coordination to iron. As will be discussed below, the energies obtained for this reaction mechanism were found to be in conflict with isotope labeling experiments and measurements of reaction rates. In the other mechanism, which is the mechanism suggested to actually occur in the enzyme, the ACV-thiol proton is proposed to stay on the thiol group or on a group in the vicinity until O_2 binds to iron. Then the same proton is suggested to be transferred to O_2 to form a hydroperoxy intermediate. This mechanism was found to be in excellent agreement with spectroscopic results as will be shown below.

The chemical model of the active site of IPNS is based on the iron complex obtained from the X-ray crystal structures.[11,17] In that model aspartate was substituted by formate and the two histidines were modeled by ammonia. In a previous study on the mechanism of manganese catalase,[37] all eight steps of that mechanism were investigated with both ammonia and imidazole as models for the actual histidines, and the results were found to be very similar from an energetics point of view, with an absolute mean deviation in the relative energies of only 1.1 kcal/mol. It was concluded that an important reason for this similarity was that ammonia did not get involved in artificial hydrogen bonding. No such bonding occurs for IPNS either and accurate results are therefore expected using ammonia ligands. This was tested for IPNS for the formation of the β-lactam ring, which was found to be a critical step as will be discussed below. For this step, the use of imidazole ligands instead of ammonia was found to lower the activation energy by 2 kcal/mol. Since formate is chemically much more similar to aspartate than ammonia is to histidine, the error obtained from using the formate model should be even smaller than that obtained for ammonia. The model used for ACV includes the most important parts of both the valine and the cysteinyl groups as shown below in the figures of the optimized structures.

The discussion of the different mechanisms investigated is organized as follows. The first reaction pathway that will be discussed is shown in Figure 4. The most striking result from that investigation is that this path gives a much too high activation energy for the cleavage of the O−O bond. This leads to a proposal of another mechanism for this step given in Figure 7, where an additional proton assists the O−O cleavage reaction. After that the problem found with the very first step of Figure 4, involving the H atom transfer from the Cys-β-carbon to O_2, is discussed, leading to the suggested mechanism shown in Figure 9. The last part of the paper is concerned with the reaction leading from the β-lactam intermediate to the thiazolidine ring of IPN.

The first step considered in this study involves the cleavage of O_2 and formation of the β-lactam ring with a simultaneous loss of a water molecule (Figure 1b). The mechanism initially investigated is shown in Figure 4. However, this mechanism is not suggested to occur in the enzyme (see further below). The reaction shown in Figure 4 is initialized by a H atom transfer from the Cys-β-carbon to the O_2 group, forming an Fe(II)-bound peroxide. The optimized structure of the modeled O_2:IPNS:Fe:ACV complex is shown as **1** in Figure 5. The cluster shown in Figure 5 is uncharged and has a quintet spin state. The spin population obtained on Fe and the O−O group is 3.77 and 0.58, respectively, while the Cys-S has a negative spin of −0.51. The rest of the spin is distributed mainly over the Fe ligands. There is also a septet state, which is energetically and structurally very similar to the quintet state. The main difference

(37) Siegbahn, P. E. M. Submitted for publication.

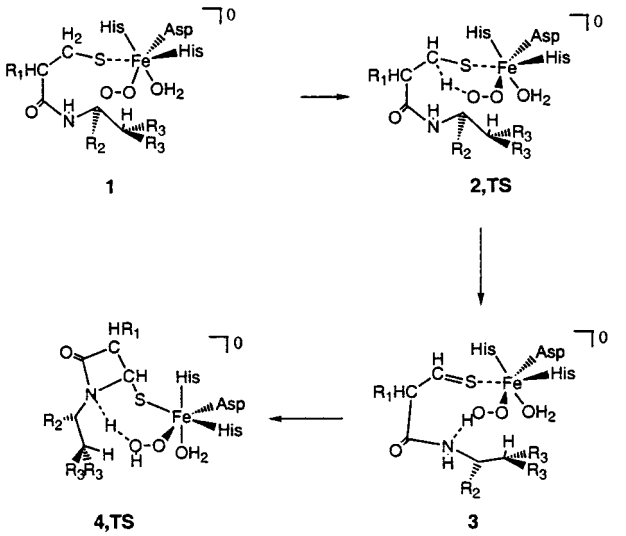

Figure 4. Reaction mechanism initially investigated for formation of the oxo-ferryl complex and the monocyclic β-lactam ring in IPNS.

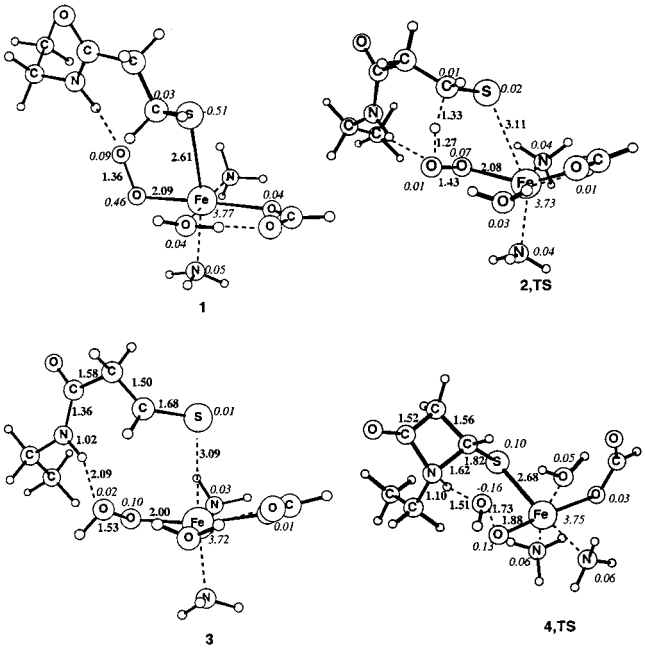

Figure 5. Geometry-optimized structures involved in the mechanism initially investigated for β-lactam ring formation in IPNS (see Figure 4). All structures are neutral. Selected bond distances (Å) are given in bold and spin-populations are given in italic.

is that all spins are ferromagnetically coupled in the septet structure. It cannot be determined from the calculations which one of the quintet and the septet states is the ground state. For the present complexes, the assignment of oxidation states on iron is complicated by the fact that spin-populations are present on the O−O and Cys-S ligands. However, a correlation between iron oxidation states and iron spin-populations has previously been obtained from calculations on several $[Fe(OH)_x(H_2O)_y]^z$ complexes, showing that a spin population of 3.7−3.8 approximately corresponds to Fe(II), of 4.0−4.2 to Fe(III), and of 3.0−3.3 to Fe(IV) using the same methods as used in the present study.[38,39] Following this scheme, the spin-population of 3.77 found on iron in **1** would indicate Fe(II).

(38) Blomberg, M. R. A.; Siegbahn, P. E. M. *Theor. Chem. Acc.* **1997**, *97*, 72−80.

(39) Blomberg, M. R. A.; Siegbahn, P. E. M. *Mol. Phys.* **1999**, *96*, 571−581.

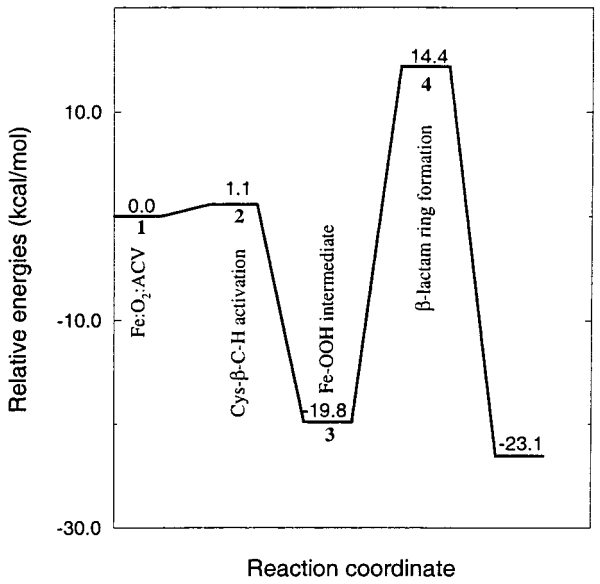

Figure 6. Potential energy surface obtained for the reaction pathway initially investigated (Figure 4) for monocyclic β-lactam ring formation.

In the geometry optimization of this structure, the distance between the Val N-H hydrogen and the dioxygen was held fixed at 1.9 Å, while all other structural parameters were optimized. The O−H distance was frozen to mimic hydrogen bonds between the substrate and the surroundings that probably would prevent the amide group from moving far away from the dioxygen group[17] to which it forms a hydrogen bond after formation of the peroxide (see further Computational Details).

Using the present model and methods, the hydrogen atom could be transferred from the Cys-β-carbon to the O−O−Fe group with an activation energy of only 1.1 kcal/mol (see Figure 6). In the optimized transition state structure shown as **2** in Figure 5, the hydrogen has a distance of 1.33 Å to the Cys-β-carbon and a distance of 1.27 Å to the dioxygen. As in the reactant, the distance between the Val N-H hydrogen and the dioxygen was frozen at a distance of 1.9 Å, while all other structural parameters were optimized.

The product of this reaction step is shown as **3** in Figure 5. In this reaction step, the distance between the Val N-H hydrogen and the hydroperoxy group was relaxed and a hydrogen bond was formed between these groups. The distance between iron and the dioxygen group decreases from 2.09 to 2.00 Å, while the O−O distance increases by 0.16 Å, from 1.36 to 1.53 Å. As this happens, the Cys-S forms a double bond to the Cys-β-carbon, shown by the shortening of the distance to this carbon of 0.36 Å. Due to the double bond formed to Cys-S, the interaction between Cys-S and Fe becomes weaker, giving a change of the distance between these two atoms of 0.48 Å, from 2.61 Å in **1** to 3.09 Å in **3**. Furthermore, the spin population on S of −0.51, present in the reactant, disappears. This reaction step was found to be exothermic by 19.8 kcal/mol. The spin-population on Fe of 3.72 indicates an Fe(II) oxidation state (see above), with one covalent bond to the peroxy group and one bond to the carboxylate group.

In the next step of the mechanism shown in Figure 4, the distal oxygen of the HOO−Fe moiety becomes protonated to form the second water molecule of the catalytic cycle, followed by formation of a bond between the Cys-β-carbon and the Val-nitrogen, thus closing the monocyclic β-lactam ring. Initially, attempts were made to move the proton directly from the Val-nitrogen to the peroxy group, with a simultaneous closure of the ring. However, the transition state obtained for such a reaction path (**4** of Figure 5) gave an energy barrier of 34.2 kcal/mol, which is much too high (see Figure 6). The energetic effect of using the more realistic imidazoles as models for the IPNS histidine ligands instead of ammonia was found to be only −1.9 kcal/mol. The barrier obtained for this mechanism is thus at least 15 kcal/mol higher than what should be expected for this step. This discrepancy between experimental and calculated barriers is much larger than the errors expected from using the present methods. It is therefore concluded that a different mechanism must be applicable for this step.

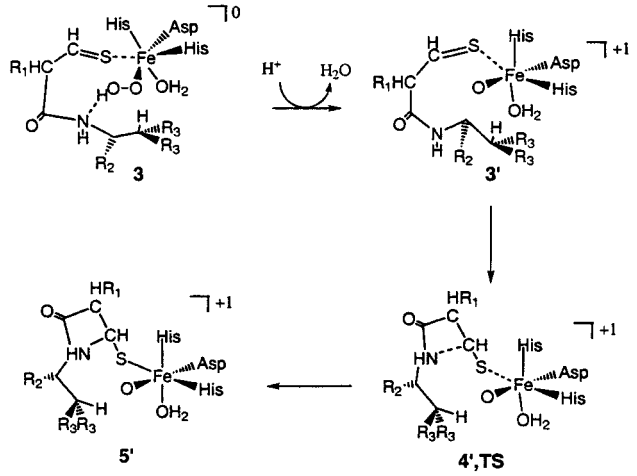

Figure 7. Second reaction mechanism investigated for β-lactam ring formation from a neutral hydroperoxy complex in IPNS. Structure **3** is neutral. All other structures have net charges of +1 (indicated by primed numbers).

If, instead, the proton is transferred to peroxide from outside and the ring closure occurs after the water is formed, giving a mechanism shown in Figure 7, the barrier can be significantly lowered. When a proton was placed on the peroxide group, a full geometry optimization resulted in dissociation of the water molecule and formation of an iron-oxo intermediate without passing a barrier. The positively charged cluster formed in this step is shown as **3′** in Figure 8. In this structure the distance between the Val-N nitrogen and the Fe-O oxygen was frozen at the same value of 4.0 Å as was obtained for **3**, to avoid unrealistic distortions, hindered by the hydrogen bonds in the actual protein (see further Computational Details). The iron-oxo distance obtained is 1.65 Å and the spin obtained on the oxo ligand is 0.69. This reaction step (**3** → **3′**) leads to a change of the iron oxidation state from Fe(II) to Fe(IV) as revealed both from the change of the number of covalent bonds to iron and the change of the iron spin, which is 3.7 in the neutral peroxide complex (**3**) and 3.0 in the positively charged iron-oxo structure (**3′**). The spin populations obtained on iron are consistent with the general experience for Fe(II) and Fe(IV) complexes using the same methods[38,39] (see above).

The final step of the mechanism shown in Figure 7 is the monocyclic ring closure. The transition state obtained for this reaction step is shown as **4′** in Figure 8. The energy obtained for the transition state (**4′**) is +13.3 kcal/mol relative to the energy obtained for **3′**. When the ring closure is completed the Val-N proton is proposed to leave the active site. The formation of the β-lactam ring leads to a regeneration of the cysteinyl thiol having single bond distances to the Cys-β-carbon and iron of 1.90 and 2.38 Å, respectively. Throughout the reaction step **3′** → **5′**, iron has the oxidation state Fe(IV) as revealed by the spin-populations on iron shown in Figure 8 (see the discussion above). The last step of the β-lactam ring formation reaction (**3′** → **5′**) was found to be endothermic by 8.0 kcal/mol.

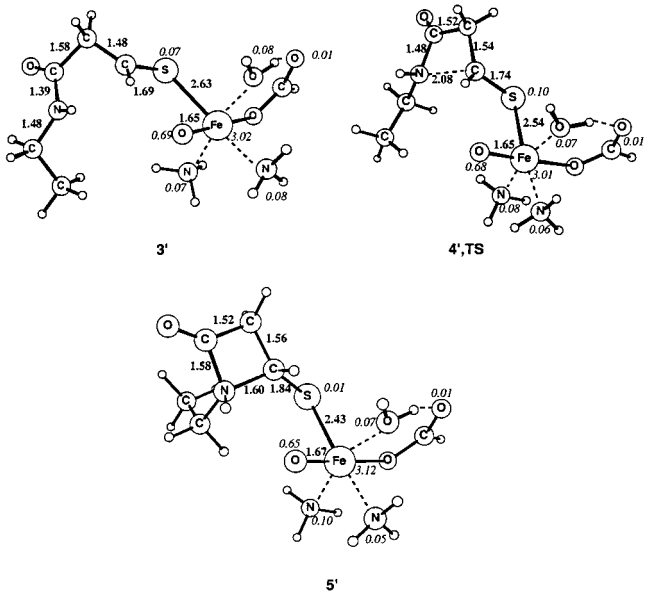

Figure 8. Geometry-optimized structures with net charges of +1, obtained for intermediates involved in the mechanism shown in Figure 7. Selected bond distances (Å) are given in bold and spin-populations are given in italic.

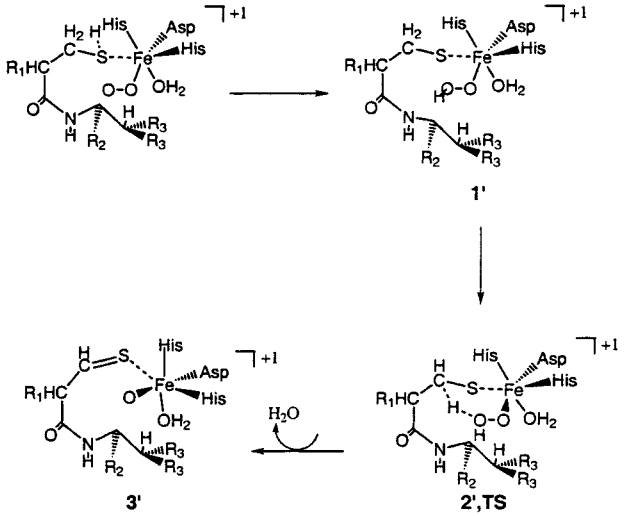

Figure 9. Suggested reaction mechanism for formation of the oxo-ferryl complex of IPNS. Complex **3′** is then proposed to be followed by **4′** of Figure 7.

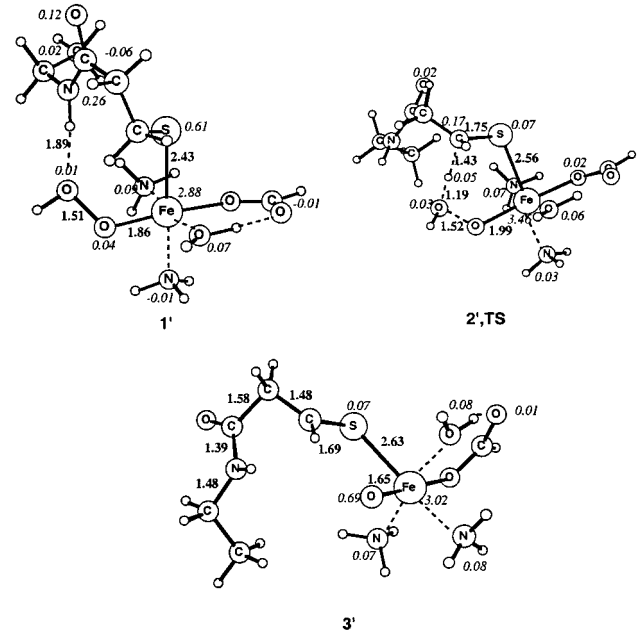

Figure 10. Geometry-optimized structures with net charges of +1 for intermediates involved in the mechanism shown in Figure 9. Selected bond distances (Å) are given in bold and spin-populations are given in italic.

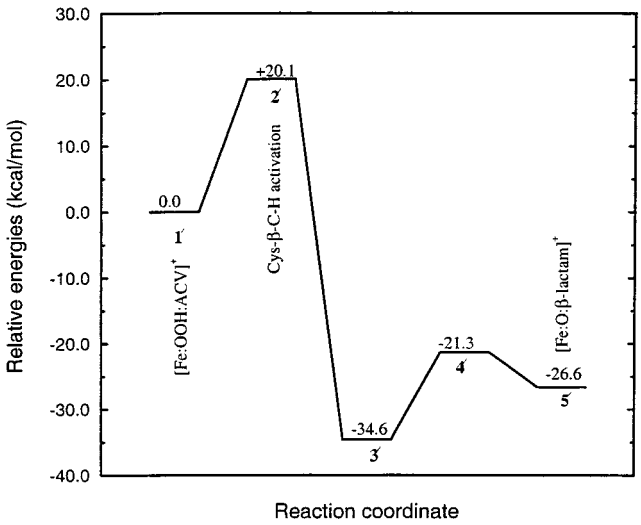

Figure 11. Potential energy surface obtained for the monocyclic β-lactam ring formation in the IPNS reaction cycle.

The above results indicate thus that an outside proton is needed for formation of the β-lactam ring. The high barrier of 34.2 kcal/mol obtained for the reaction step **3** → **4** of Figure 4 involving a proton transfer from the Val-nitrogen to the peroxy group suggests the alternative pathway shown in Figure 7, where a barrier of only 13.3 kcal/mol was obtained. However, also the first reaction step, **1** → **3** of Figure 4, needs to be modified, see below.

When the energetic results obtained for the oxy-ferryl formation step (**1** → **3** in Figure 4) are analyzed closer it can be noted that the very small reaction barrier of 1.1 kcal/mol obtained for this step is inconsistent with spectroscopic data. Isotope labeling experiments show that kinetic isotope effects are present for both the Cys-β-C-H hydrogen and the Val-β-C-H hydrogen, indicating that rate-determining C−H activations occur at these two sites.[18] Both steps should therefore have significant reaction barriers of similar size, around 17 kcal/mol. The barrier obtained for the Cys-β-C-H hydrogen step of only 1.1 kcal/mol yielding an error of more than 10 kcal/mol is far outside the expected error bars. This situation is the opposite of the one described above, where a too high barrier was obtained. In that case a mechanism with a lower barrier had to be found, but in this case the step with the too low barrier has to be prevented instead. To prevent the transfer of the Cys-β-C-H hydrogen, there appears to be no other possibility than blocking the peroxide position by another proton. This means that there must be another reaction pathway also for the first step of the reaction, involving the formation of the oxo-ferryl from the dioxygen complex (**1** → **3** in Figure 4). One such alternative mechanism for formation of the oxo-ferryl is shown in Figure 9.

In this mechanism, the proton present on the ACV thiol group is proposed to remain at this group or possibly be transferred to a nearby group when ACV coordinates to iron. When O_2

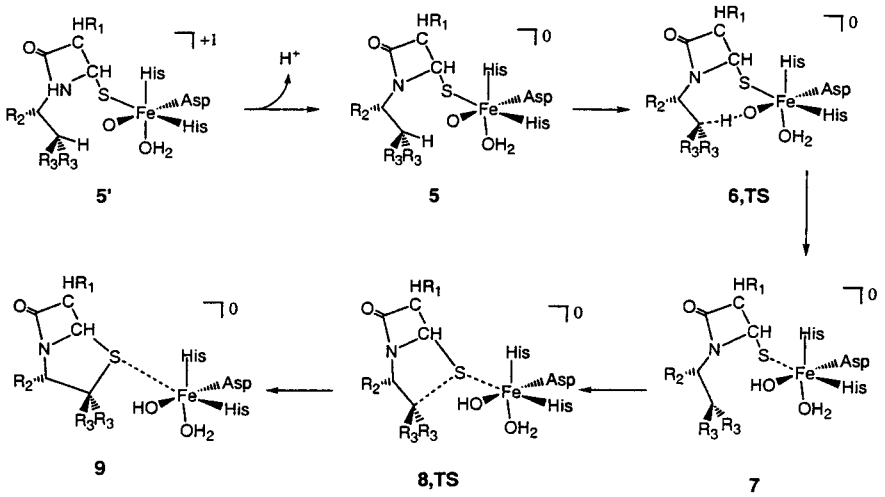

Figure 12. Mechanism investigated for the bicyclic ring formation in IPNS.

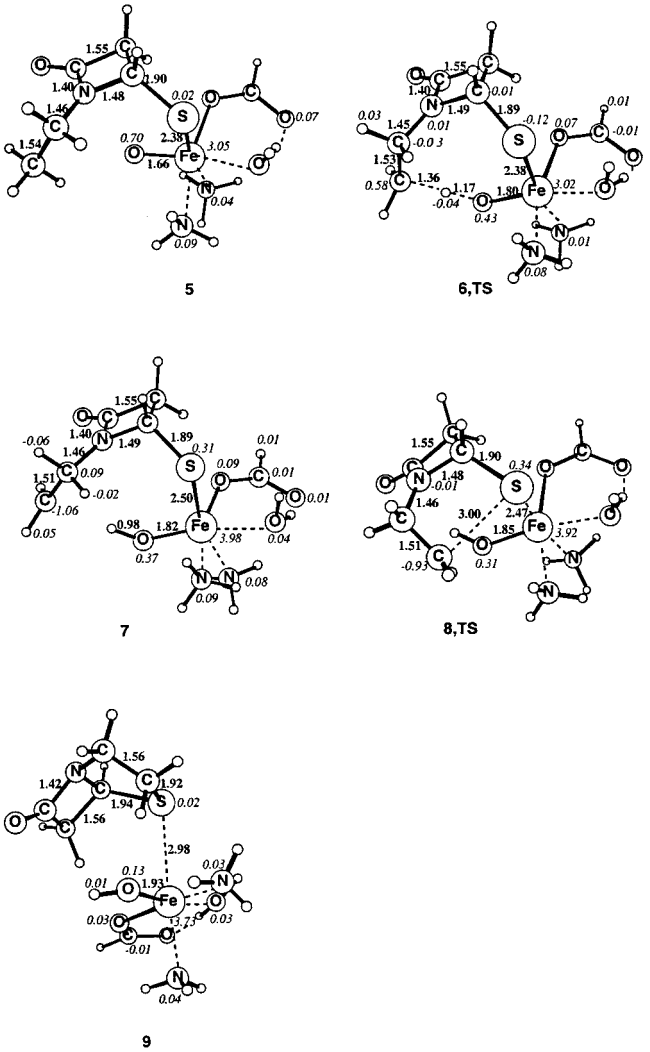

Figure 13. Geometry-optimized structures obtained for intermediates suggested to be involved in the bicyclic ring formation in IPNS. All structures are neutral. Selected bond distances (Å) are given in bold and spin-populations are given in italic.

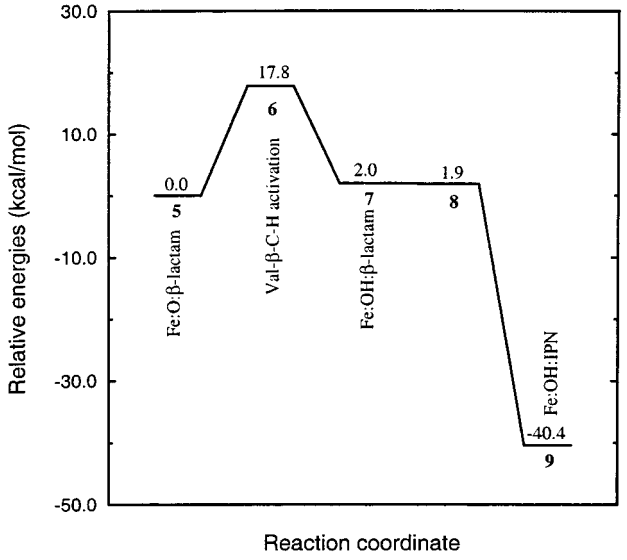

Figure 14. Potential energy surface obtained for IPN formation from the β-lactam ring in IPNS.

binds to the cluster, the thiol proton is suggested to be transferred to O_2 to form a hydroperoxy intermediate. The geometry-optimized model structure for the product formed after proton transfer from the thiol to the dioxygen is shown as **1′** of Figure 10. This structure has a net charge of +1. The O−O distance of 1.51 Å obtained for **1′** is significantly longer than the distance of 1.36 Å obtained in structure **1** shown in Figure 5. The distance between iron and the dioxygen group is 2.09 Å in **1**, compared to 1.86 Å in **1′**. Furthermore, the spin population on iron decreases after proton transfer to the dioxygen resulting in a spin population of 2.88, indicating Fe(IV). There is no spin on the oxygens. Instead, the remaining spin is distributed over the whole cluster. From structure **1′**, a hydrogen atom transfer from Cys-β-carbon to the HOO group should then lead to loss of one water molecule and, in a subsequent step, the formation of the β-lactam ring.

To find the transition state for the H atom transfer between the Cys-β-carbon and the HOO group, the O−H and the O−O bond distances were frozen at different values and all other structural parameters were optimized. From this two-dimensional search of the potential energy surface it was found that the reaction coordinate corresponds to an energy path where the H atom transfer occurs in the initial step and only when the H atom is at a very short distance from the HOO group is the O−O bond cleaved and water formed. In the highest energy point along the H atom transfer coordinate a Hessian was computed. Using this Hessian, a transition state geometry optimization was performed. In the geometry optimization the distance between the Val-nitrogen and the oxygen of the water

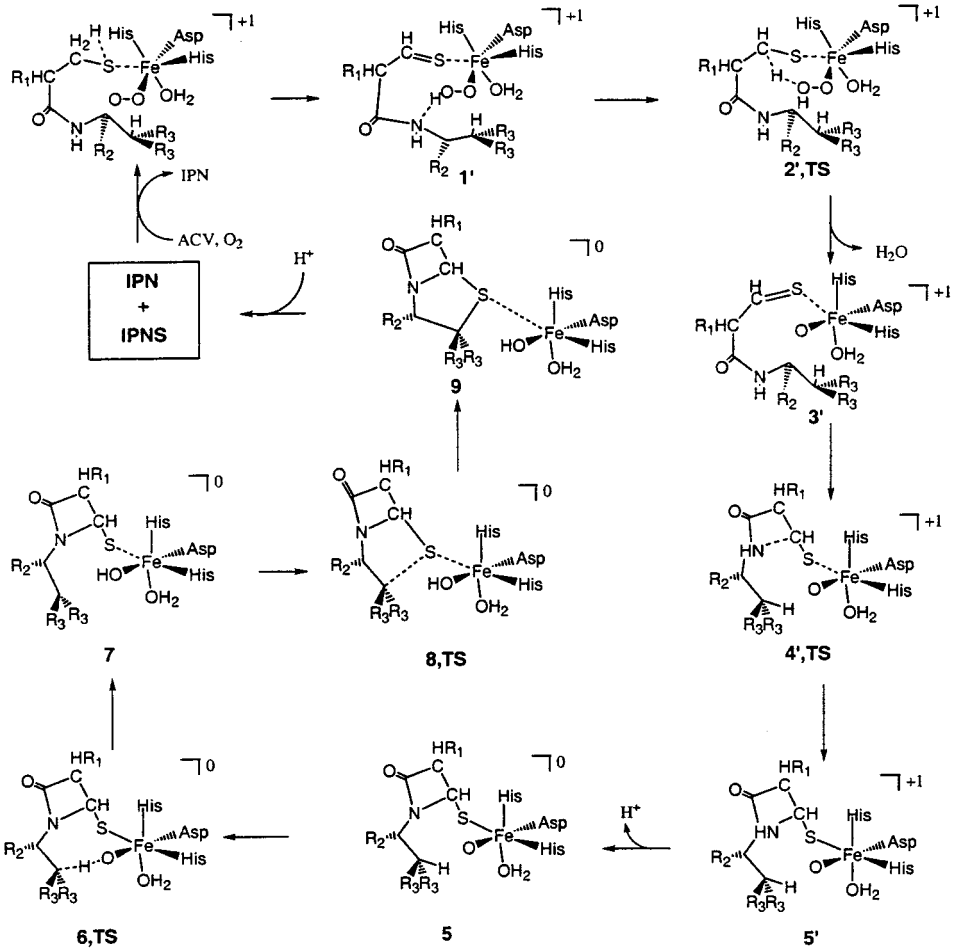

Figure 15. Catalytic mechanism finally proposed for isopenicillin N formation based on the present calculations.

being formed was frozen at the value obtained for this distance in the reactant (**1′**) to avoid large structural changes of the ACV analogue (see further Computational Details). The converged transition state is shown as **2′** in Figure 10. In the transition state, the distance between carbon and hydrogen is stretched to a value of 1.43 Å and the distance between the hydrogen and oxygen is 1.19 Å. The O−O distance is almost unchanged in the transition state with a value of 1.52 Å, compared to 1.51 Å in the reactant. The Fe−O distance is elongated from a value of 1.86 Å in the reactant to a value of 1.99 Å in the transition state. Furthermore, the spin on iron changes from 2.88 to 3.46, indicating that iron becomes slightly reduced in the transition state. The reaction barrier was determined to be 20.1 kcal/mol, a value in rather good agreement with the catalytic rate of 4.6 s^{-1}, which indicates a barrier of about 17 kcal/mol. The exothermicity of this step was found to be 34.6 kcal/mol, and the product is shown as **3′** in Figure 10. The iron−oxo distance obtained is 1.65 Å and the spin obtained on the oxo ligand is 0.69. The spin on iron is 3.02, indicating a regeneration of Fe(IV).

On the basis of the results reported above, the formation of the monocyclic β-lactam ring from the dioxygen complex is thus suggested to occur in 5 steps. In the first step the dioxygen is protonated by the thiol group of ACV or a nearby group. Then, the Cys-β-C-H activation occurs with a simultaneous formation of water and an oxo-ferryl compound (Figure 9). After that, the monocyclic ring is formed and simultaneously, or immediately after, the Val-N nitrogen is deprotonated (Figure 7). In Figure 11, the potential energy surface for the proposed monocyclic ring formation is shown. The energy value used for the β-lactam ring intermediate in Figure 11 is obtained for the protonated form (**5′**). However, the system is likely to gain energy from deprotonation of the Val-N nitrogen by a nearby group, which would stabilize this point. A stabilization of the β-lactam intermediate relative to the value shown in Figure 11 is actually required since the reaction can experimentally be interrupted after the formation of the monocyclic ring when the substrate analogue ACMC is used.[18,19,22] Unfortunately, a determination of the energy gain from deprotonation requires much larger models, and this question therefore has to be postponed to the future.

The last step of the reaction involves the closure of the thiazolidine ring, which completes the formation of the bicyclic structure of IPN (Figure 1c). This reaction step was found to occur in two substeps. In the first of these, the Val-β-C-H hydrogen is transferred to the oxo ligand on iron, creating a hydroxo intermediate (**5**−**7** of Figure 12). In the transition state for this step (**6** of Figure 13), the migrating hydrogen has a distance of 1.36 Å to the Val-β-carbon where a spin-population of 0.58 appears. The spin-population on the oxo ligand in the transition state is 0.43, compared to the value of 0.70 obtained for the reactant (**5**). Furthermore, the Fe−O distance of 1.80 Å in the transition state is elongated compared to **5**, where this distance is 1.66 Å. The reaction barrier obtained is 18.4 kcal/mol, which is a value comparable to the activation energy of 20.1 kcal/mol obtained for the Cys-β-C-H activation and also with the experimental barrier of 17 kcal/mol. These results are thus in good agreement with interpretations of kinetic isotope effects observed in deuterium labeling studies,[18] where both steps are suggested to be partially rate-determining. When the

hydrogen atom transfer is completed (**7**), the Val-β-carbon has a negative spin-population of −1.06. The spin of 3.98 obtained on iron and the presence of three single bonds to this atom are consistent with an Fe(III) oxidation state.

The formation of the bicyclic structure (**7**−**9**) is then completed by the bond formation between the Val-β-carbon and the Cys-sulfur. At the level of geometry optimization a very small barrier of 0.2 kcal/mol was obtained, but the energy point of the transition state (**8**) was lowered by 0.3 kcal/mol relative to the reactant (**7**) when the larger basis set was used, indicating an activation energy close to zero for this step. The formation of the bicyclic ring was found to be very exothermic, giving a reaction energy of 42.4 kcal/mol. The energy profile obtained for formation of IPN from the monocyclic ring is given in Figure 14. In the product shown as **9** in Figure 13, IPNS is weakly interacting with IPN, with a distance between iron and the Cys-sulfur of 2.98 Å. Two covalent bonds and an iron spin population of 3.73 indicates a reduction from Fe(III) to Fe(II) in the reaction step **7**−**9**. The catalytic cycle is then closed by a proton transfer to the hydroxyl ligand present in **9** and a coordination of Gln 330.

IV. Conclusions

The mechanism previously proposed[18] for IPN formation catalyzed by IPNS has been investigated using the DFT-B3LYP method. The energetic results obtained in the present study suggest that the dioxygen becomes protonated in an initial step of the catalytic cycle, probably by the proton originally present on the ACV thiolate. The proposed reaction mechanism from the dioxygen intermediate back to the resting state of IPNS is shown in Figure 15. After the proton transfer to the dioxygen, the Cys-β-C-H bond is activated resulting in formation of water and an oxo-ferryl intermediate (**1′**−**3′**). This step was found to have a barrier of 20.1 kcal/mol, which is the highest barrier obtained along the whole potential surface as shown in Figure 11. In a subsequent step, the monocyclic β-lactam ring is formed. Simultaneously, or immediately after, the Val-N nitrogen of the ring is deprotonated, giving **5**. The other significant barrier of the reaction is obtained for the Val-β-C-H cleavage to form the iron-hydroxo complex, regenerating IPNS in its original form. The activation energy obtained for this reaction step (**5** → **7**) is 18.5 kcal/mol. Thus, the two barriers associated with the Cys-β-C-H cleavage and the Val-β-C-H cleavage are of almost equal size. The activation energies obtained agree well with the maximum catalytic rate of 4.6 s^{-1} measured for IPNS in solution, which approximately corresponds to a barrier of 17 kcal/mol.[16] They further agree with spectroscopical results, showing that these two C−H activations both are rate-determining. The last reaction step **7** → **9**, which includes the closing of the bicyclic ring, was found to be very exothermic. The exothermicity obtained for closing the thiazolidine ring is 42.4 kcal/mol, giving an energy of −62.9 kcal/mol for the modeled OH:IPNS:Fe:IPN complex and a free water molecule relative to the energy obtained for O_2:IPNS:Fe:ACV. Since the total exothermicity of the catalytic cycle for the substrate (without the iron complex) is 58.0 kcal/mol most of this energy is thus obtained in the closing of the thiazolidine ring.

JA001103K